Nucleic Acids Research, 2025, **53**, gkaf763
https://doi.org/10.1093/nar/gkaf763
Computational Biology

Peripheral heterochromatin tethering is required for chromatin-based nuclear mechanical response

Ali Göktuğ Attar[1,2], Jarosław Paturej[3], Ozan S. Sarıyer[4], Edward J. Banigan[5,*], Aykut Erbaş[1,3,*]

[1]UNAM - National Nanotechnology Research Center and Institute of Materials Science & Nanotechnology, Bilkent University, 06800 Ankara, Turkey
[2]School of Life Sciences, École Polytechnique Fédérale Lausanne, CH-1015 Lausanne, Switzerland
[3]Institute of Physics, University of Silesia, 40-007 Katowice, Poland
[4]School of Arts and Sciences, Pîrî Reis University, Tuzla 34940, Istanbul, Turkey
[5]Institute for Medical Engineering and Science and Department of Physics, Massachusetts Institute of Technology, Cambridge, MA 02139, United States

[*]To whom correspondence should be addressed. Email: aykut.erbas@unam.bilkent.edu.tr
Correspondence may also be addressed to Edward J. Banigan. Email: ebanigan@mit.edu

Abstract

The cell nucleus is a mechanically responsive structure that governs how external forces affect chromosomes. Chromatin, particularly transcriptionally inactive heterochromatin, resists nuclear deformations through its mechanical response. However, chromatin also exhibits liquid-like properties, casting ambiguity on the physical mechanisms of chromatin-based nuclear elasticity. To determine how heterochromatin strengthens nuclear mechanical response, we performed polymer physics simulations of a nucleus model validated by micromechanical measurements and chromosome conformation capture data. The attachment of peripheral heterochromatin to the lamina is required to transmit forces directly to the chromatin and elicit its elastic response. Thus, increases in heterochromatin levels increase nuclear rigidity by increasing the linkages between chromatin and the lamina. Crosslinks within heterochromatin, such as HP1α proteins, can also stiffen nuclei, but only if chromatin is peripherally tethered. In contrast, heterochromatin affinity interactions that may drive liquid–liquid phase separation do not contribute to nuclear rigidity. When the nucleus is stretched, gel-like peripheral heterochromatin can bear stresses and deform, while the more fluid-like interior euchromatin is less perturbed. Thus, heterochromatin's internal structure and stiffness may regulate nuclear mechanics via peripheral attachment to the lamina, while also enabling nuclear mechanosensing of external forces and external measurement of the nucleus' internal architecture.

Graphical abstract

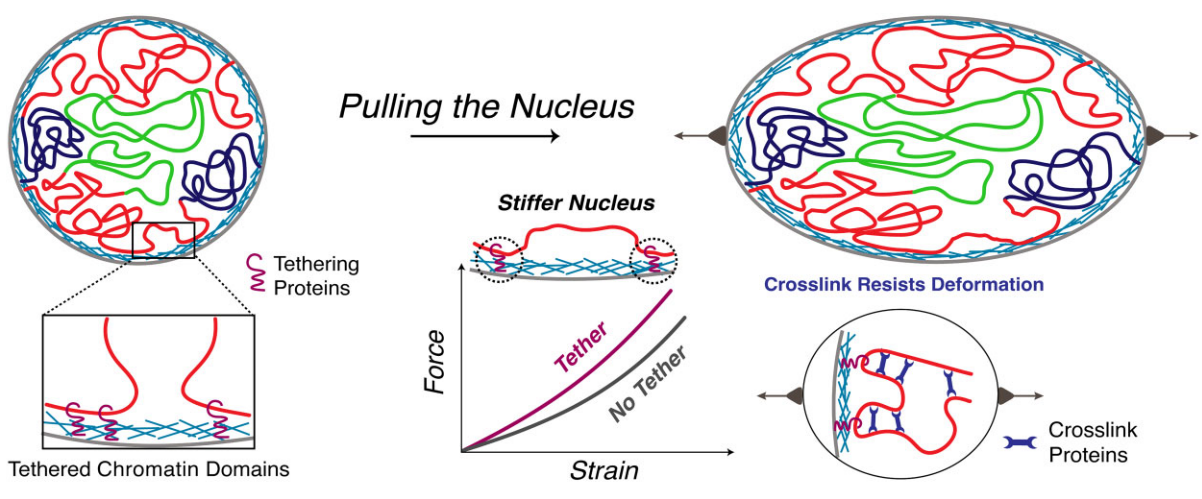

Received: April 17, 2025. **Revised:** July 17, 2025. **Editorial Decision:** July 18, 2025. **Accepted:** July 31, 2025

Introduction

Cells are constantly subjected to mechanical stresses due to forces transmitted across whole tissue, individual cell interactions with the extracellular environment, constricted migration, internal cytoskeletal reorganization, and myriad other factors [1, 2]. Mechanical stresses deform nuclei [1–3], alter chromatin spatial organization [2, 4–7], modulate gene transcription [4, 8–10], increase DNA damage [3, 11–15], transform or redistribute epigenetic marks [4, 5, 7, 16], and consequently, affect cell fate and identity [1, 3, 4]. These mechanobiological effects require the internal chromatin to sense the exterior of the nucleus or cell. In turn, they require physical mechanisms that couple disparate length scales such that mechanical forces acting at the nucleus scale (microns) can be propagated to the length scales of chromatin segments (tens of nanometers) [2, 17]. However, questions persist about the internal architecture and material state of chromatin [18], so the physical mechanisms underlying chromatin-based nuclear mechanical response remain unclear.

Experimental observations of chromatin's material properties and physical organization suggest that chromatin can be liquid- and solid-like. *In vitro*, chromatin can exhibit properties of either state, depending on ionic and biochemical conditions [19, 20]. *In vivo*, single nucleosomes [21, 22] and telomere-bound proteins [23] exhibit liquid-like dynamics, while viscoelastic measurements made by atomic force microscopy (AFM) on cell surfaces [24], magnetically pulling a sub-micron chromatin locus [25], or inducing interfacial forces by condensation [26] suggest that chromatin may be described as a viscoelastic fluid. However, rheological measurements using half-micron magnetic beads suggest that chromatin is a polymer gel [27]. Furthermore, micromanipulation experiments stretching cell nuclei demonstrate that heterochromatin is a major contributor to the elastic response of the nucleus and similarly suggest gel-like chromatin [28–31]. These differing observations might be reconciled by the inhomogeneous chromatin elasticity observed in deformation microscopy [16, 32], optical tweezers [33], AFM [24, 34], and localized thermal perturbation [35] experiments.

Heterochromatin has distinct features that enforce spatial inhomogeneity within the nucleus and contribute to nuclear mechanics. Heterochromatic regions are enriched in histone methylation and chromatin-crosslinking proteins, such as HP1α, both of which bolster nuclear stiffness [28–31, 36]. Furthermore, methylation and chromatin bridging by HP1α may drive spatial segregation by phase separation [37–39], which may further strengthen chromatin and nuclei [40, 41]. Spatial segregation is further enforced in most cells by an array of proteins that peripherally tether chromatin to the nuclear lamina, including emerin, LBR, LAP2, PRR14, and lamin A, among others [42–48]. In turn, heterochromatin localization at the periphery may protect the genome and facilitate nuclear mechanosensing by mechanically responding to applied stresses and stabilizing nuclear structure [49, 50].

Supporting this idea, cells dynamically alter heterochromatin levels, composition, and localization in response to various mechanical stimuli. In cyclically contracting cardiomyocytes, H3K9me3-marked heterochromatin accumulates at the nuclear periphery, while passive cardiomyocyte nuclei exhibit a uniform pattern of H3K9me3 [16]. Similarly, cell migration and associated nuclear deformations are associated with increases in H3K27me3 and peripheral H3K9me3 heterochromatin [5, 7, 15, 51–53]. In both cardiomyocytes and migrating cells, dense heterochromatic regions undergo larger deformations [16, 32] or changes in chromatin contacts [5, 6] than presumably softer euchromatic regions. Consistent with this protective effect, heterochromatin may form in sufficiently soft nuclei to inhibit DNA damage [3, 30]. However, in stiffer epidermal stem cell nuclei, applied forces have also been observed to reduce H3K9me3 heterochromatin, which decreases nuclear stiffness [3, 4]; this fluidizing effect inhibits DNA damage, perhaps because chromatin is less fragile in that scenario [2, 3]. Thus, heterochromatin is not only regulated by forces but also has a critical role in sensing, transmitting, and responding to them.

Three-dimensional spatial modeling of chromatin suggests several possible mechanisms underlying different aspects of heterochromatin organization and structure. Polymer models with nonspecific affinity interactions between heterochromatic subunits and between heterochromatin and the lamina can capture compartmentalization and spatial localization of heterochromatin observed in chromosome conformation capture data (3C, Hi-C, Micro-C, etc.) and imaging experiments [47, 54–56]. However, it was suggested that these models cannot explain nucleus stretching experiments [28]. Simulation models of chromatin as a uniformly crosslinked polymer gel linked by specific bonds to the nuclear lamina can recapitulate nuclear mechanical response [28, 31, 57], but are at odds with the nonuniform spatial distribution of heterochromatin [45] and the elasticity measured in chromatin locus pulling experiments [25]. Together, these models raise the questions of what internal structures enable heterochromatin levels to increase nuclear stiffness and how heterochromatin fulfills its apparent mechanical function.

To investigate the physical mechanisms by which heterochromatin contributes to nuclear stiffness and mechanosensing, we measure nuclear force response in a coarse-grained polymer physical model of the cell nucleus that includes epigenetic features of chromatin, chromatin-binding proteins, and a mechanically realistic nuclear lamina. We explored several scenarios: (i) heterochromatin that is unconstrained by specific linkages (i.e. neither internal crosslinking nor peripheral tethering to the lamina), (ii) heterochromatin that is constrained by internal crosslinks but not peripheral tethering, and (iii) heterochromatin that is tethered, with or without internal crosslinks. Our results revealed that heterochromatin enhances nuclear rigidity only when tethered to the nuclear lamina, facilitating the propagation of mechanical stress across the nucleus. Without chromatin tethering, heterochromatin failed to bolster nuclear stiffness even with strong crosslinking. Peripheral heterochromatin levels were directly linked to nuclear stiffness, with reduced heterochromatin tethering resulting in softer nuclei. Increasing heterochromatin levels further constrains heterochromatin through new lamina tethering and/or chromatin crosslinking, both of which increase nuclear stiffness. Additionally, we observed that lamina tethering and crosslinking direct mechanical deformations to the heterochromatin and lamina-associated domains (LADs). Our work thus uncovers a critical role for heterochromatin-lamina linkages in facilitating chromatin-based nuclear mechanical response and demonstrates how heterochromatin structure and mechanics are regulated to facilitate mechanosensing or protect the genome when nuclei are stressed and deformed.

Materials and methods

We performed molecular dynamics simulations of nuclei stretched by axially applied tensile forces using a polymer model of chromosomes inside of a polymeric lamina shell [28, 31, 57, 58]. Below, we briefly describe the simulation setup and procedure, and additional details are provided in the Supplementary data.

Chromatin polymer

Triblock copolymers model eight 240 Mb chromosomes. Each copolymer comprises $N = 6002$ monomeric subunits, where the two ends are telomeres, followed by 1000 subunits at one end that are designated as constitutive heterochromatin and 5000 subunits representing genomic loci capable of forming A- and B-type compartments (euchromatin and facultative heterochromatin, respectively; Fig. 1A), which are assigned based on chromosomes 1 and 2 of mouse rod cells (four of each) [47]. Subunits represent 40 kb of chromatin, each of size $b = 1\sigma \approx 150$ nm, where σ is the unit simulation length. Adjacent polymer subunits are connected by inextensible bond potentials. Interaction strengths between different chromatin types and between heterochromatin and shell subunits were swept and selected to model chromatin phase separation as in previous work [47, 55, 58, 59].

Chromatin polymers are initially compact, chromatid-like structures placed randomly near the nuclear center, and they are subsequently relaxed (Fig. 1A). Chromatin fills the spherical volume and segregates into heterochromatin-rich and poor domains, as expected [43, 45, 47]. In simulations with heterochromatin tethering and/or crosslinks, permanent (unbreakable) tethering to the shell and/or crosslinking are introduced after the last time step of equilibration. Crosslinks were assigned to subunits in contact after equilibration. Each heterochromatin subunit is crosslinked with probability $P_c = 0.2$ (unless noted) to a maximum of two others that are in contact (i.e. $r_H \leq 2.5\sigma$). Chromatin subunits within $r_L \leq 2.5\sigma$ of the lamina were connected with a probability P_t to one lamina subunit, with $P_t = 1.0$ unless noted. For models of different levels or architectures of heterochromatin, perturbations to the control structure are introduced after the initial equilibration. In simulations altering heterochromatin fraction, f, only facultative heterochromatin is changed. Crosslinks and tethers are assigned after a change in the heterochromatin fractions; the numbers of tethers and crosslinks correlate with the alteration in facultative heterochromatin levels.

Nuclear lamina shell

We modeled the lamina as an elastic, spherical polymeric shell using a bead-spring network of 15 000 monomeric subunits (Fig. 1A). This network mimics the nuclear lamina meshwork [60–63] and reproduces the stress-strain responses of isolated nuclei in micromanipulation experiments [28, 57, 64]. Lamina subunits were randomly positioned on the surface of a sphere with an initial radius $R_i = 42\sigma$. Subunits were connected by inextensible bond potentials, with each subunit forming $5 \leq n_{\mathrm{bond}} \leq 8$ bonds. After chromatin polymer relaxation, the shell radius is reduced to a starting radius of $R_s = 32\sigma$. After further relaxation of the composite polymer-shell structure, the shell relaxes to $R_0 \approx 29\sigma$, achieving a chromatin volume fraction of $\phi \approx 23\%$ [65] and a nuclear diameter of ≈ 10 μm.

Force spectroscopy simulations

Nuclei were stretched by applying axial pulling forces at two opposing poles as in micromanipulation experiments [28, 57] (Fig. 1B). To mimic partial aspiration by the micropipettes, 80 subunits from each pole ($|y| \geq 28\sigma$) were randomly selected at the start of the simulation to be pulled (Supplementary Fig. S1). Pulling was achieved by harmonic spring potentials, and forces exerted by these potentials were recorded. Springs with stiffness $K = 20k_BT/\sigma^2$ were initially positioned at $y_0 = \pm 60\sigma$ (with the nucleus centered at the origin), and each was moved away at constant velocity $v_{\mathrm{pull}} = 0.1\sigma/\tau$, where $\tau = 500$ time steps (Fig. 1B and Supplementary Fig. S2). The pulling force is given by $F = \pm K(v_{\mathrm{pull}}t - y_0)$, where t is the elapsed time. No qualitative changes were observed with variations in pulling velocity or spring constant (Supplementary Fig. S2). Each pulling simulation ran for 2×10^5 time steps, resulting in strains up to $\lambda \equiv \Delta L/R_0 \approx 80\%$. The built-in *fix smd* algorithm within the LAMMPS MD package was utilized [66]. Ovito is used for visualization of trajectories [67]. Ten replicates were performed per simulation condition.

Chromatin contact frequencies

To compute chromatin contact frequencies, as measured in Hi-C experiments [47, 68], we counted subunits within $r \leq r_c = 2.5\sigma$ at each simulation frame. $P(s)$ curves were computed for facultative heterochromatin and/or euchromatin only. Similarly, chromatin contacts with the lamina were computed as a contact index, which was taken to be 1 for subunits within $r_L \leq 2.5\sigma$ of the lamina and 0 otherwise. Measurements were averaged over 10 simulation replicates, using 10 configurations (snapshots) from each simulation just before stretching to 30% strain, and, unless noted, 110 configurations just after stretching.

Results

Chromatin governs nuclear force response to small to moderate deformations

Previous force spectroscopy experiments with isolated nuclei established the distinct mechanical contribution of chromatin to nuclear rigidity, independent of lamin proteins [28, 29, 31, 33, 69]. We first used force spectroscopy simulations to assess whether our multiblock copolymer simulation model captures the contribution of chromatin to nuclear stiffness.

Simulated nuclei were progressively stretched via forces applied to the lamin subunits at opposite poles (Fig. 1C; see the "Materials and methods" section). Forces were applied to lamins by spring potentials whose centers were moved apart at a constant velocity, mimicking the experimental pulling protocol [28]. Stretching simulations of a chromatin-filled polymeric shell produced a strain-stiffening force response, with the measured force increasing more abruptly for larger strains (Fig. 1C, gray), as in experiments [28, 33]. Thus, our model is consistent with the nuclear force response to dynamic stretching.

To confirm that chromatin is essential for nuclear stiffness at small deformations, we stretched empty polymeric shells (i.e. without the chromatin polymer). These simulations modeled treatment by the enzyme MNase, which digests chromatin. The empty shell produced a minuscule force response, with an effective spring constant (local slope of the force-extension curve), k_{nuc}, almost an order of magnitude lower

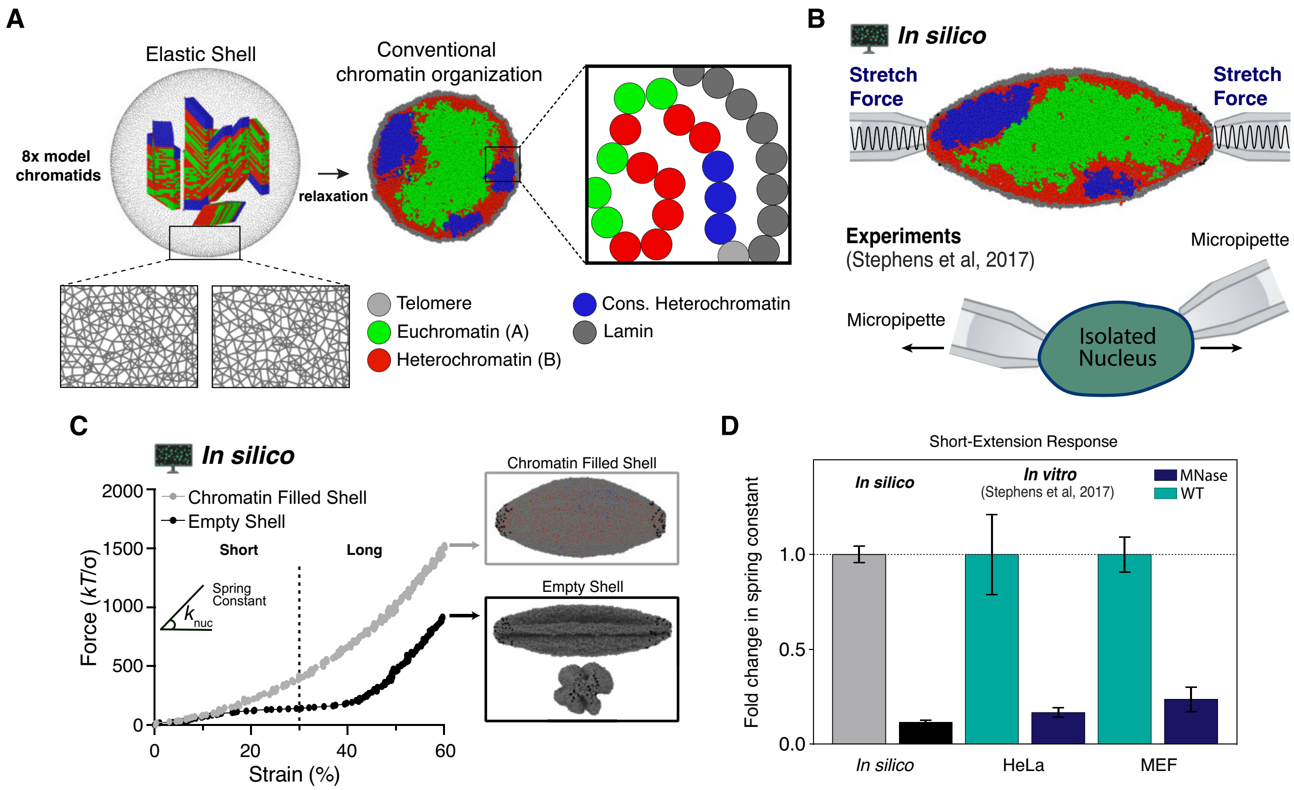

Figure 1. Heteropolymer simulation model recapitulates cell nuclear mechanical response. (**A**) Eight chromatid-like structures are relaxed into a phase-separated mixture of constitutive and facultative heterochromatin (blue and red) and euchromatin (green) within a polymeric lamina (gray). (**B**) Simulation snapshot with a schematic illustration of applied axial forces (top) and illustration of corresponding micromanipulation force spectroscopy experiment. (**C**) Representative force-strain curves measured in simulations of a chromatin-filled nucleus (gray) and an empty polymeric shell (i.e. only the lamina; black). Insets show simulation snapshots of the deformed morphologies; the empty shell inset also shows lamina buckles in a rotated view. (**D**) Fold change in short-extension spring constant from wildtype or typical simulation nuclei (turquoise or gray, respectively) to MNase-treated nuclei or empty polymeric shells (navy blue or black) regimes in experiments [28] and simulations.

than that of the chromatin-filled nucleus. This behavior persisted up to strains of ∼40% (Fig. 1C, black), in agreement with previous experiments and simulations [28, 33, 57]. Beyond 40% strain, deformation to the lamina increases the stress and alignment in lamin–lamin bonds along the direction of the applied force [28, 57] (Supplementary Fig. S3). Deformed empty nuclei have smaller cross-sectional dimensions, shrink, and exhibit longitudinal buckles (Fig. 1C), as in previous simulations and experiments [57]. Therefore, the chromatin polymer is critical for a robust mechanical response to small strains.

Peripheral localization and phase separation of heterochromatin alone do not increase nuclear rigidity

Heterochromatin is paramount to chromatin-based nuclear rigidity [3, 28, 29, 31, 36]. Heterochromatin is thought to be established, maintained, and peripherally localized by polymer phase segregation [20, 37, 38, 47, 54, 55, 59, 70–74] and interactions with the nuclear lamina [42, 43, 46–48, 75, 76]. Therefore, we investigated how alterations to heterochromatin phase separation impact nuclear stiffness.

We tested whether increasing the prevalence of the heterochromatic phase would increase nuclear stiffness, similar to experimental observations [28, 29, 31]. We randomly converted heterochromatin subunits into euchromatin or vice versa to tune total heterochromatin content to a prescribed level. This procedure also altered the peripheral localization of heterochromatin because heterochromatin subunits have a nonspecific affinity to the lamina [47, 58]. Surprisingly, we found that nuclear force response does not increase with increasing heterochromatin content (Fig. 2A–C), but rather, slightly *decreases*. This is due to the larger polymer osmotic pressure of the less compact euchromatin phase [77]. This reinforces the notion that the origin of chromatin-based stiffness in cell nuclei is not osmotic pressure alone [28]. Together, our findings suggest that heterochromatin phase separation and peripheral localization do not govern nuclear rigidity on their own.

Since heterochromatin should strengthen nuclear force response, we speculated that the heterochromatin affinity interactions in our simulations might be too weak. However, despite increasing the heterochromatin-lamina affinity fourfold, the effective nuclear spring constant, k_{nuc}, did not significantly change (Fig. 2D). Furthermore, k_{nuc} remained insensitive to alterations in heterochromatin levels (Supplementary Fig. S4). Similarly, heterochromatin self-affinity did not affect the nuclear spring constants for a broad range of affinities (Fig. 2E). Even in simulations with strong affinity interactions, the heterochromatin phase could move along the nuclear periphery (e.g. inset to Fig. 2D) and/or internally rearrange as the nucleus deformed, without altering the number, and thus, the total energy, of heterochromatin-lamina and heterochromatin-heterochromatin contacts. We conclude that while heterochromatin-lamina attractions and heterochro-

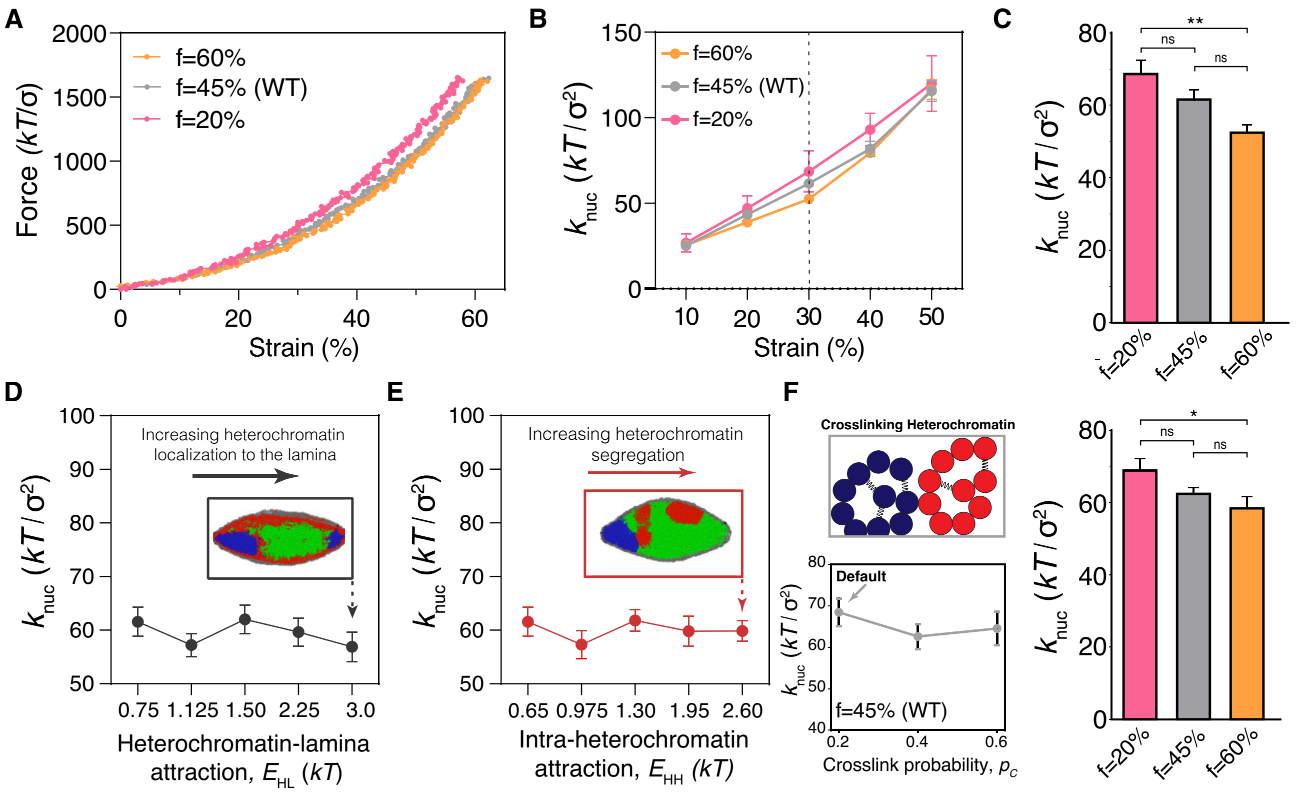

Figure 2. Effects of heterochromatin microphase separation and internal structure on nuclear mechanical response. (**A**) Representative force-strain curves for nuclei with different fractions, *f*, of facultative heterochromatin, in nuclei with nonspecific affinity interactions between heterochromatin and the lamina. (**B**) The nuclear spring constant averaged over 10 replicates for various facultative heterochromatin levels, *f*, at different strains. (**C**) Nuclear spring constants computed from the slope of the force-strain curves at 30% strain. ** indicates p-values $p < 0.01$, while ns denotes not significant. (**D**) Nuclear spring constants at 30% strain as a function of the heterochromatin-lamina subunit attraction energy, E_{HL}, and (**E**) the intra-heterochromatin subunit attraction energy, E_{HH}. Inset images show representative snapshots of nuclear deformations and spatial organization of euchromatin (green), facultative heterochromatin (red), and constitutive heterochromatin (blue) contained within the nuclear lamina (gray). (**F**) Top left: schematic illustration of crosslinking within heterochromatin. Constitutive (blue) and facultative (red) heterochromatin may crosslink to other heterochromatin subunits of the same type. Bottom left: spring constants, k_{nuc} at 30% strain for different levels of crosslinking, set by the crosslink probability, P_c. Right: bar plot showing spring constants versus heterochromatin fraction, *f*, with $P_c = 0.2$ such that the total number of crosslinks increases with *f*. Data are shown as mean ± standard error of the mean (SEM). Statistical significance is assessed by one-way ANOVA followed by a post-hoc Tukey's HSD test for pairwise comparisons. * denotes $p < 0.05$ and ** denotes $p < 0.01$.

matin self-affinity may govern mesoscale chromatin phase separation, they do not provide a robust mechanical coupling between nuclear deformation and heterochromatin and, therefore, do not promote nuclear rigidity.

Heterochromatin-based nuclear stiffness cannot be explained by chromatin crosslinking alone

We next turned to a mechanism previously shown to bolster chromatin-based nuclear rigidity in both experiments and simulations: chromatin–chromatin crosslinking [31, 40]. To model crosslinks, such as HP1α [78, 79], we introduced permanent bonds between heterochromatin subunits. Surprisingly, heterochromatin crosslinking slightly decreased nuclear stiffness in force spectroscopy simulations, similar to the effects of affinity interactions (Fig. 2F), and this trend is independent of heterochromatin levels (Supplementary Figs S5 and S6). This shows that externally applied forces that generate small deformations (<30% strain) do not deform the chromatin segments constrained by crosslinks, so crosslinks do not increase nuclear rigidity in this scenario. Therefore, crosslinks alone do not explain the chromatin-based nuclear mechanical response. This result suggests that the model lacks a key mechanical component required to generate a force response.

Tethering heterochromatin to the lamina is required for heterochromatin-driven nuclear force response

We sought to understand why alterations to heterochromatin polymer structure and organization did not elicit a strong change in force response (Fig. 2). In our initial model, interactions between heterochromatin and the lamina were nonspecific, allowing significant chromatin mobility. However, in contrast, many cells have specific tethers between chromatin and the lamina or nuclear envelope, either through lamin A itself or lamina- or envelope-associated proteins, including LBR, LAP2, emerin, and PRR14, among others [43, 44, 46, 48, 75, 80, 81]. Therefore, we tested whether specifically tethering heterochromatin to the lamina would mechanically couple heterochromatin architecture to nuclear force response.

We incorporated specific, unbreakable, stretchable heterochromatin-lamina tethers into the model (Fig. 3A; see the "Materials and methods" section) and simulated nuclear stretching. Nuclei with chromatin-lamina tethers exhibited a systematic increase in nuclear stiffness for small to moderate

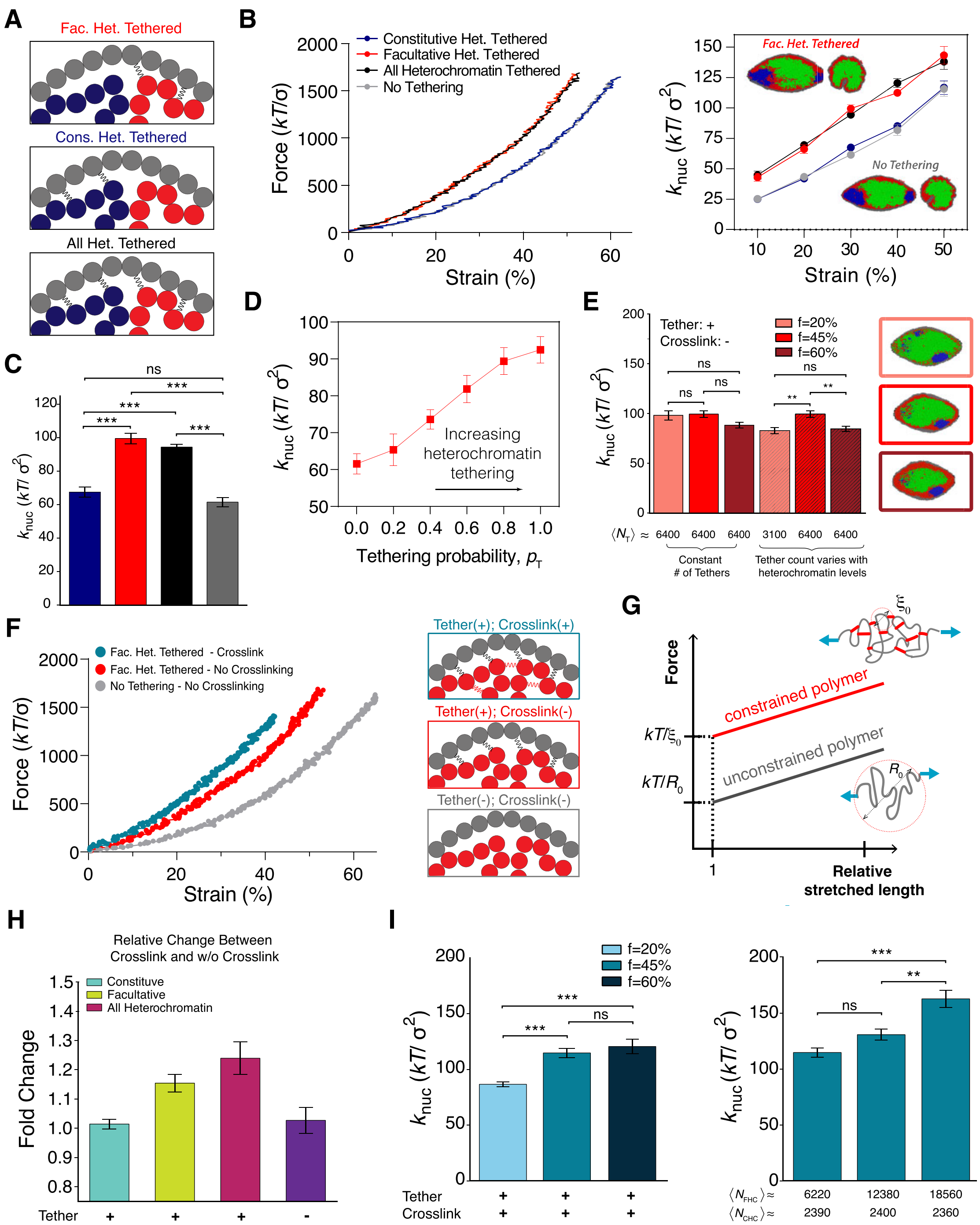

Figure 3. Nuclear mechanical effects of heterochromatin tethering and changes in tethered heterochromatin organization. (**A**) Illustrations of specific tethering of heterochromatin to the lamina. (**B**) Left: Representative force-strain curves for nuclei with and without tethering of peripheral heterochromatin to the lamina. Right: Spring constants, k_{nuc}, as a function of strain. (**C**) Effective spring constants, k_{nuc}, at 30% strain, obtained from at least 10 independent force spectroscopy simulations. (**D**) Nuclear spring constant as a function of facultative heterochromatin tethering probability, P_T. (**E**) Nuclear spring constant for various levels of heterochromatin, f, where $f = 45\%$ is the control case. The mean number of tethers, $\langle N_T \rangle$, is either increased probabilistically (see the "Materials and methods" section) with f or held constant, as indicated by the numbers below each bar. Simulation snapshots are shown for increasing tethering number. (**F**) Left: Representative force-strain curves for nuclei with and without heterochromatin crosslinking in the presence or absence of facultative heterochromatin tethering. Right: Illustrations of these scenarios. (**G**) Schematic force-strain plot and illustration of expected scaling of force response as a function of relative stretched polymer length. Heterochromatin crosslinks act as constraints that decrease the length of stretchable polymer segments. (**H**) Fold change in effective nuclear spring constant from untethered and uncrosslinked scenario (purple) for nuclei with specific tethering and crosslinking only within different types of heterochromatin: constitutive (turquoise), facultative (yellow), and all (red). (**I**) Effective spring constants with different levels of crosslinked heterochromatin with lamina tethering. Left: k_{nuc} with tethered and crosslinked heterochromatin for different heterochromatin fractions, f, with crosslinking probability $P_c = 0.2$ such that the number of crosslinks increases with f. Right: k_{nuc} with tethered and crosslinked heterochromatin at fixed f, but with crosslinking levels determined by different crosslinking probabilities, P_c. Mean quantities of facultative and constitutive heterochromatin crosslinks, $\langle N_{FHC} \rangle$ and $\langle N_{CHC} \rangle$, respectively, are listed beneath each bar. Bars are mean ± SEM. Statistical significance is assessed by one-way ANOVA followed by a post-hoc Tukey's HSD test for pairwise comparisons. * denotes $p < 0.05$, ** denotes $p < 0.01$, and *** denotes $p < 0.001$.

deformations (Fig. 3B–D and Supplementary Figs S7 and S8), consistent with previous research [31, 80, 82]; the effective nuclear spring constant for small deformations is two-fold higher in nuclei with chromatin tethering than in those without. Furthermore, in simulations with moderate amounts of heterochromatin tethering ($P_t < 1$), nuclei exhibited an intermediate force response (Fig. 3D). Visual inspection reveals that the bulk spatial organization of the chromatin phases after deformation is similar in both cases (Fig. 3B, inset). These observations demonstrate that the mechanical coupling imposed by heterochromatin tethers, but not peripheral heterochromatin localization alone, stiffens nuclei.

Between the two types of tethers linking heterochromatin to the lamina, those associated with facultative heterochromatin are the main contributors to nuclear rigidity (Fig. 3A–C). The facultative heterochromatin phase has a larger interaction area with the lamina, so it has a larger number of tethers and mechanically couples the entire lamina. In contrast, tethering only constitutive heterochromatin (Fig. 3A) to the shell does not increase the nuclear spring constant (Fig. 3B and C). Therefore, although constitutive heterochromatin more strongly phase separates and peripherally localizes in the model [47, 58], it contributes less to nuclear mechanics. Together, our results indicate that one mechanism for heterochromatin-induced nuclear stiffness is the increase in chromatin-lamina tethering, which might coincide with expanding the lamina-associated heterochromatin phase.

Chromatin-lamina tethering links heterochromatin levels to nuclear rigidity

To test whether linkages between chromatin and the lamina also directly connect nuclear mechanical properties and heterochromatin levels, we repeated the force spectroscopy simulation measurements on nuclei with specific heterochromatin-lamina linkages. With tethering to the lamina, reducing heterochromatin levels resulted in a systematic decrease in nuclear rigidity compared to the control case with “normal” heterochromatin levels (Fig. 3E). Increasing heterochromatin also resulted in a slight reduction in k_{nuc}. Nonetheless, in contrast to the model without chromatin tethering (Fig. 2A–C), a $\sim$25% decrease in heterochromatin can explain the reported decrease in the nuclear spring constant induced by inhibition of heterochromatic epigenetic modifications by methyltransferases in experiments [28–31] (Fig. 3E).

Heterochromatin-driven changes in nuclear stiffness were due to two factors: (i) chromatin condensation altering polymer osmotic pressure (as in Fig. 2C) and (ii) changes in the number of tethers to the nuclear lamina. Decreasing heterochromatin fraction reduces the number of chromatin-lamina tethers, which decreases nuclear stiffness, despite a concurrent increase in polymer osmotic pressure due to chromatin decondensation. However, increasing heterochromatin fraction from $f = 45\%$ to $f = 60\%$ also slightly decreases k_{nuc} because the peripheral tethering is already saturated at $f = 45\%$, but chromatin further condenses with this change. Consistent with this idea, if the total number of tethers is held constant, the model reproduces the trend observed without tethering (Fig. 2C): heterochromatin increases reduce nuclear stiffness (Fig. 3E).

Once again, these results indicate that nonspecific interactions between nuclear components are insufficient to produce the experimentally observed changes to nuclear rigidity. Instead, as shown by the stretching of chromosomal segments between tethered sites, it is the physical constraints of specific sites to the lamina that contribute to nuclear rigidity (Supplementary Figs S7 and S8). Therefore, the physical bridging of heterochromatin to the lamina provides the mechanical coupling needed to enable heterochromatin to respond to forces applied to the nucleus. Heterochromatin-driven nuclear stiffening can arise indirectly through heterochromatin’s effect on the quantity of chromatin-to-lamina linkages.

Heterochromatin crosslinks directly contribute to nuclear force response when chromatin is tethered to the lamina

To determine whether heterochromatin can regulate nuclear stiffness through its own biophysical properties, we considered a model in which heterochromatin has internal crosslinks in addition to specific tethers to the nuclear lamina (Fig. 3F and G, and Supplementary Fig. S9). In the presence of chromatin-lamina tethers, nuclear rigidity is sensitive to the degree of heterochromatin crosslinking, unlike simulations without tethers (Fig. 2F, G, and I). With tethering, nuclei stiffen with increasing levels of heterochromatin crosslinking, even when the number of chromatin-lamina tethers is held constant (Fig. 3H and I). This is consistent with previous simulations with crosslinks throughout all chromatin [31]. Furthermore, with tethering and crosslinking, elevating the amount of heterochromatin can stiffen the nucleus because this perturbation also increases the total level of intra-chromatin crosslinking (Fig. 3I).

These observations sharply contrast with results for simulations without chromatin-lamina tethering (Fig. 2F). Therefore, while heterochromatin crosslinking may provide an important component of nuclear mechanical response, the effect depends on tethering to the lamina. Altogether, chromatin tethering to the lamina enables nuclear mechanosensing by providing the critical links for chromatin to “sense” applied forces and external factors to “see” the internal physical organization and structure of the nucleus.

Nuclear stretching increases lamina-associated heterochromatin

Our simulations indicate that mechanical communication between the nuclear periphery and interior arises due to physical constraints imposed by chromatin-lamina tethers. We next asked how these constraints affect force transmission into the nuclear interior and reorganize chromatin. To address this question, we performed *in silico* versions of DamID [83, 84] and Hi-C [68] by computing lamina-chromatin contacts and chromatin contact maps before and after nuclear stretching.

These analyses reveal small but systematic differences in peripheral heterochromatin rearrangement in nuclei with and without tethering to the lamina. With heterochromatin tethered to the lamina, nuclear deformations result in expansion of LADs, as measured by heterochromatin-lamina contacts (Fig. 4A and B). These new LADs form at the expense of chromatin–chromatin contacts, as shown by a systematic change in contact frequency (Supplementary Fig. S13). In contrast, without peripheral heterochromatin tethering, chromatin contacts with both the lamina and other chromatin segments are largely unaltered by nuclear deformations (Fig. 4A and Supplementary Figs S10–S12). These measurements show that, in our model, chromatin-lamina tethering allows external mechanical perturbations to be transmitted into peripheral heterochromatin and spatially reorganize the genome.

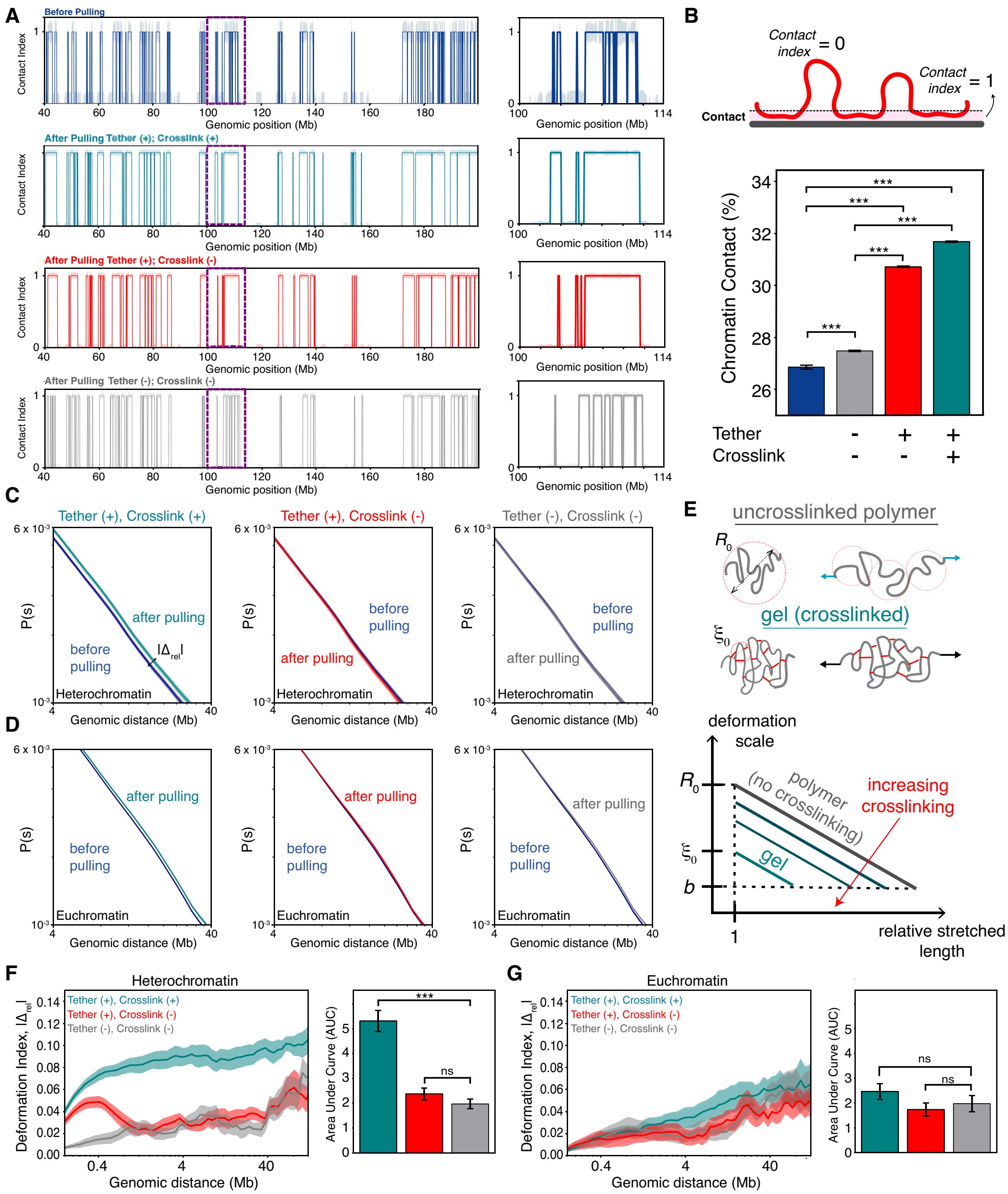

Figure 4. Chromatin-lamina tethering and crosslinking direct chromatin reorganization during nuclear deformation. (**A**) Simulated DamID of a 160 Mb region of chromosome 1 showing contact index of genomic sites before stretching (blue) and after 30% axial strain in nuclei with tethering and internal crosslinking of facultative heterochromatin (turquoise), tethering facultative heterochromatin without crosslinking (red), and untethered and uncrosslinked heterochromatin (gray). The contact index is 1 for chromatin subunits in contact with the lamina and 0 otherwise. The solid line shows a representative example, while shading indicates standard error. Right: 14 Mb snippet showing zoomed-in view of chromatin-lamina contacts for the region boxed on the left. (**B**) Top: Illustration of contact index. Bottom: Percentage of heterochromatin in contact with the lamina genome-wide, defined as distance $r < 2.5\sigma$, before stretching (navy blue bar) or after pulling to 30% strain in nuclei with and without heterochromatin tethering and/or crosslinking (gray, red, and turquoise). * indicates $p < 0.05$, ** indicates $p < 0.01$, and *** indicates $p < 0.001$. (**C**) Chromatin contact frequencies as a function of genomic distance for intra-heterochromatin contacts for the genomic distances of 4–40 Mb, before and after 30% nuclear strain for nuclei with both lamina tethering and heterochromatin crosslinking (left), tethering but no crosslinking (center), or neither tethering nor crosslinking (right). $|\Delta_{rel}| = |(P_{after}(s) - P_{before}(s))/P_{before}(s)|$ indicates the absolute relative change in $P(s)$ after deformation. (**D**) Chromatin contact frequencies as a function of genomic distance for intra-euchromatin contacts before and after nuclear deformation for different tethering and crosslinking scenarios. (**E**) Log-Log scaling plot showing the expected size of the internal deformation in chromatin as a function of strain for crosslinked ("gel") and uncrosslinked ("unconstrained") polymers. Illustrations show length scales over which deformations occur due to the presence or lack of constraining linkages. (**F**) Left: Absolute relative change, $|\Delta_{rel}|$, in heterochromatic contacts as a function of genomic distance after deformation of nuclei with both lamina tethering and heterochromatin crosslinking (turquoise), tethering but no crosslinking (red), or neither tethering nor crosslinking (gray). Right: Bar plot showing the total absolute relative change, summed over all genomic distances. (**G**) Absolute relative change, $|\Delta_{rel}|$, in euchromatic contacts as a function of genomic distance, with a bar plot showing the total change in contacts. Statistical significance is assessed by an unpaired, two-sided Student's t-test.

Remarkably, tethering and crosslinking of peripheral heterochromatin alter how the internal organization of both euchromatin and heterochromatin responds to nuclear deformations. In nuclei with unconstrained chromatin (no tethering and crosslinking), genomic contacts are only minimally perturbed by nuclear deformations of 30% strain (Fig. 4C–G). In contrast, with tethering and crosslinking, nuclear deformation alters heterochromatic contacts compared to nuclei with unconstrained chromatin, thus transmitting mechanical signals to chromatin segments. Tethering alone also alters heterochromatic contacts, but to a lesser degree and only for shorter-ranged contacts (<1 Mb). In euchromatin, deformation has a smaller effect on genomic contacts. Nonetheless, increased force transmission with peripheral chromatin crosslinking and tethering leads to a small additional alteration to euchromatic contacts. This difference disappears at large genomic distances (Supplementary Fig. S11). Together, these observations suggest that the regulation of heterochromatin and its connections to the nuclear lamina allow the nuclear interior to sense external forces while also protecting euchromatin from mechanical disruptions.

Discussion

Using force to see inside nuclei

Forces can be used to biophysically perturb cell nuclei, but because nuclei deform in response, forces can also measure nuclear mechanical properties. Changes in heterochromatin within the nucleus alter nuclear rigidity [3, 28–31, 36, 41, 85]; therefore, forces can be used to detect the physical state of the nuclear interior, allowing us to "see" inside the nucleus. Using an established polymer simulation model (Fig. 1) [28, 31, 57, 58], we find that physical linkages between peripheral heterochromatin and the nuclear lamina are essential for force transmission into the nucleus and external sensing of the properties of the nuclear interior (Fig. 3). This finding complements the biological findings of the importance of peripheral chromatin tethering for mechanotransduction and sequestration and silencing of genes [42, 43, 45, 46, 48, 76, 81].

Our molecular dynamics simulations of nuclei stretched as in micromanipulation experiments [28, 33, 64, 69] reveal the physical mechanism of heterochromatin-based nuclear rigidity. We find that heterochromatin levels, self-affinity, and crosslinking alone cannot regulate nuclear mechanical response (Fig. 2). Peripheral heterochromatin must also be physically linked to the lamina, so that forces can be elastically transmitted from the lamina to chromatin. In the absence of tethering, simulated nuclei are softer (Figs 2 and 3). With tethering, heterochromatin crosslinking, but not non-specific self-affinity, bolsters nuclear stiffness (Fig. 3). Heterochromatin levels are important to the extent that they govern the quantity of chromatin-to-lamina linkages and intra-chromatin crosslinks (Fig. 3). Consistently, heterochromatin tethering and crosslinking facilitate reorganization of LADs and force transmission to the nuclear interior in response to nuclear deformations (Fig. 4). We note that our results are general to different types of force application. In simulations of uniaxial compression, under which the nucleus is compressed by plates along one axis but allowed to expand in the perpendicular directions, we observed similar effects of heterochromatin tethering and crosslinking on nuclear stiffness (Supplementary Fig. S13). Thus, our model establishes how forces applied to the cell nucleus can be transmitted into the genome to potentially sense and transduce mechanical signals, and how regulation of peripheral heterochromatin might alter the mechanobiological response of the nucleus.

Limitations of the model

Unlike in living cells, the simulated chromosomes and lamina are elastic structures of beads and springs with fixed topology. Therefore, the applied forces do not irreversibly alter nuclear architecture. Permitting rupture of bonds or dissociation of lamins from the nuclear envelope [86] could modulate how forces are transmitted to chromatin and increase the viscous response at the expense of nuclear elasticity. In addition, the simulated shell-like structure of the lamina precluded robust formation of wrinkles that could potentially unfold. Such structures could result in additional strain stiffening if unfolding of the lamina facilitates additional chromatin-lamina tethers [87, 88].

We also note that the focus on isolated nuclei here (Fig. 1) and in previous work may ignore important effects of cytoskeletal and extracellular forces on nuclear shape [11, 12, 29, 89–95]. Supporting this notion, in previous models, increased chromatin tethering [96, 97] or association of the heterochromatin phase with the envelope [58] resulted in large fluctuations, bulges, wrinkles, or other disruptions to nuclear shape. We hypothesize that in a non-isolated or mechanically active environment, nuclear stiffness from chromatin-lamina tethering (Fig. 3) might stabilize nuclear shape. Consistently, previous simulations with active forces on the envelope induced blebs in nuclei with abnormally, but not uniformly, patterned chromatin-lamina tethering [98]. Thus, while our model captures nuclear elasticity, the current version may not fully reproduce how chromatin-lamina tethering can differentially alter nuclear shape depending on the mechanical environment.

Tethering links chromatin to nuclear force transmission and response

Chromatin-lamina tethering profoundly impacts nuclear mechanical response in simulations. In experiments, nuclear mechanics generally exhibits two regimes: chromatin-dominated stiffness in response to small nuclear deformations and lamin-dominated stiffness in response to large deformations [28, 33, 64, 69, 99]. Heterochromatic histone modifications, such as H3K9me3 and H3K27me3, stiffen cell nuclei, while histone hyperacetylation leads to softer nuclei [3, 28–31, 36, 69, 99–101]. Although chromatin modifications alter nuclear stiffness independently of lamins, our results indicate that the physical coupling of chromatin to the lamina is essential for these effects.

Peripheral linkages transmit forces applied to the cell nucleus directly to chromatin to elicit a resistive force response. This could not be achieved if the chromosomes acted as unconstrained polymers. Tethers constrain the polymer chromosomes so that lamina (and nuclear) deformations reposition tethered loci, thus stretching the chromosomal segments between tethered sites (Fig. 1). With untethered chromosomes, forces are transmitted globally across the entire chromatin-lamina interface, and unconstrained polymer chromosomes reposition and internally reorganize without significantly stretching chromosomal segments (Fig. 4) [77]. This phenomenon has been observed in *Schizosaccharomyces pombe* nuclei depleted of LEM-domain protein orthologs Heh1 and Heh2, which tether chromatin to the nuclear envelope [80]. Nuclei in these cells exhibited larger shape fluctuations and lower-viscosity response to applied forces, consistent with reduced nuclear stiffness and increased chromatin flow. Similarly, AFM measurements showed that human bladder cancer cells depleted of the chromatin-tethering proteins SUN1/2 had reduced viscoelastic response [82]. Thus, constraints from chromatin tethering maintain the mechanical integrity and organization of the nuclear periphery by directly transmitting forces to chromatin and enabling elastic response.

Our predictions can be tested by measuring nuclear mechanical response after histone hypermethylation in cells with disrupted chromatin-lamina tethering (e.g. Sun1/2, LAP2, LBR, emerin, or PRR14 depletion or mutation). In this context, histone hypermethylation (e.g. via methylstat treatment), which normally stiffens nuclei [28–31], should have a smaller effect or even no effect on nuclear rigidity. Similarly, in mouse rod cells, which have an inverted chromatin architecture with heterochromatin in the interior due to loss of tethering by LBR [43, 47], we would expect little change in nuclear stiffness after increasing histone methylation. These experiments could test whether cells can regulate chromatin-lamina tethering as a mechanism for controlling the mechanoregulatory functions of heterochromatin.

Peripheral heterochromatin as a tethered polymer gel

An ongoing question is whether chromatin is a polymer fluid or gel [1, 18]. Current evidence suggests that chromatin mechanics is spatially inhomogeneous [32–35], which potentially reconciles evidence for gel-like chromatin [28, 31] with measurements of softer chromatin viscoelasticity [25, 33]. Our simulations suggest that peripheral heterochromatin is tethered to the lamina in a gel-like state and thus can transmit stress across length scales, but the euchromatic interior may be less constrained (i.e. no crosslinking or lower levels of crosslinking as compared to heterochromatin).

Heterochromatin tethering is necessary to recapitulate experimental findings that an increase in heterochromatin by histone methylation increases nuclear stiffness [28, 29, 31] (Figs 2 and 3). Crosslinking of peripheral heterochromatin strengthens this effect (Fig. 3). As with chromatin-lamina tethering, crosslinking within heterochromatin spatially constrains chromatin polymer segments so that forces induce stretching and elastic response rather than repositioning by viscous flow. Consistently, chromatin-bridging proteins Cbx5/HP1α and BANF1/BAF are necessary for gene stretching and transcription induced by external force [8]. Crosslinks also enable heterochromatin to stiffen cell nuclei independent of further alterations to chromatin-lamina tethering or localization (Fig. 3). Similarly, it has been shown that degrading the crosslinker HP1α weakens cell nuclei, but does not alter peripheral heterochromatin localization [31]. Thus, spatially uniform crosslinking from previous models [28, 31, 57] is unnecessary; instead, spatially nonuniform, peripheral crosslinking along with tethering is sufficient to drive chromatin-based nuclear mechanical response.

Uncrosslinked interior euchromatin (Fig. 1), in contrast, might allow the relatively soft elastic and viscous response observed in experiments probing the chromatin interior on shorter length scales [25, 26]. Spatial inhomogeneity in chromatin material properties is maintained by histone modifications and other genomically and spatially inhomogeneous patterning [45, 76, 102, 103]. Interior euchromatin exhibits histone acetylation, which leads to softer elastic response in force spectroscopy studies [28, 29, 69] and liquid-like properties for *in vitro* chromatin [19]. However, a simple uncrosslinked polymer model for euchromatin remains at odds with other observations of chromatin dynamics. Rheological measurements with magnetic beads suggest crosslinking on length scales of half a micron [27]. This may suggest an intra-chromatin crosslinking with a relatively large crosslinking length, but observations of loss of structure in “liquid chromatin” Hi-C experiments suggest linkages every few kb [104]. A model with dynamic crosslinking (a “weak gel”) [25, 77, 105–107] may better explain chromatin’s viscoelastic properties, but remains to be extensively explored in the context of chromatin mechanics.

Force transmission through chromatin tethers and nuclear function

Force transmission through chromatin-lamina linkages is important for proper mechanotransduction of physical stresses into biochemical processes [1, 46]. Experiments using magnetic beads to apply forces to mammalian cells have shown that external forces can be transmitted to chromatin, stretch individual genes, and elevate gene expression [8, 108]. These effects depend on chromatin-lamina linkages, such as SUN1/2 and emerin. Our polymer simulations show that chromatin tethers are necessary for force transmission and activation of chromatin’s elastic response (Figs 3 and 4). This hints that nuclear mechanical properties could potentially guide the transduction of mechanical cues into biochemical and gene regulatory activity.

Remarkably, our analyses revealed that tethering to the lamina leads to large deformations of heterochromatin during nuclear strain. We observe this effect despite comparatively small alterations in euchromatin organization (Fig. 4). This defied our initial expectation that applied forces would induce larger deformations and changes in chromatin contacts in the more flexible euchromatin than in the stiffer heterochromatin. However, the simulations are consistent with experimental observations of genomes altered by nuclear deformations. In Hi-C experiments with cells that migrated through pores smaller than the nuclear diameter (5 μm), a few percent of all genomic regions switched between euchromatic A- and heterochromatic B-type compartments, as defined by chromatin contacts [5, 6]. Switches from B to A were observed more frequently, possibly indicating significant changes in B, and the relative frequency of chromatin contacts within B compartments was lower after migration. Similarly, in simulations of nuclei deformed by axial tension, peripheral heterochromatin tethering combined with heterochromatin crosslinking favored changes in heterochromatin contact frequencies at $\sim$1 Mb scales (Fig. 4). These alterations occurred because tethering and crosslinking facilitated force transmission through heterochromatin. These findings are consistent with deformation microscopy imaging showing that denser chromatin and peripheral H3K9me3-marked heterochromatic regions undergo larger strains than lower density, transcriptionally active euchromatic regions during cardiomyocyte contraction [16, 32]. We conclude that physical linkages not only stiffen nuclei but also redistribute strain.

Consequently, regulation of heterochromatin through both crosslinking and peripheral heterochromatin may be essential to mechanobiological responses to external forces. Our observations of force transmission through the nucleus suggest that polymer physical constraints, such as heterochromatin tethering and crosslinking (Fig. 4), could be mechanistically important to nuclear mechanosensing [1, 8, 46, 108]. Complementarily, tethering is necessary to detect the internal chromatin architecture via external mechanical perturbations (Fig. 3). This tethering promotes heterochromatin-based nuclear rigidity, which can protect the genome from damage [30]. However, the corresponding increase in force transmission can increase DNA damage [3, 94]. Thus, softening of nuclei by ATM-dependent reduction of heterochromatin upon DNA damage may be an adaptive response to fluidize chromatin and prevent further force transmission [85, 94]. Furthermore, the balance between mechanical protection and force transmission may depend on the composition (e.g. lamin A level) and overall rigidity of the nucleus [2, 3], as well as the scale of deformation (Fig. 4 and Supplementary Fig. S11). Our model suggests that cells may tune these competing mechanical effects through the regulation of heterochromatin quantities, crosslinking, and tethering to the lamina.

Acknowledgements

We thank Andrew Stephens for fruitful discussions.

Author contributions: A.E. conceptualized the study, A.G.A. performed simulations and data analysis. E.J.B., A.G.A., and A.E. discussed/interpreted the results and wrote and edited the manuscript. A.E., O.S.S., and J.P. performed the scaling calculations. All authors participated in reviewing and discussing the manuscript.

Supplementary data

Supplementary data is available at NAR online.

Conflict of interest

None declared.

Funding

E.J.B. acknowledges support from the National Institutes of Health (NIH) Common Fund 4D Nucleome Program (UM1HG011536). This work has been supported by the Council of Science and Technology of Turkey (TUBITAK) grant no 122F309 and the National Science Center (NCN), EU's H2020 Programme and MSCA grant agreement no. 945339, Poland [Grant Polonez Bis No. 2021/43/P/ST3/01833].

Data availability

The data generated for this study are freely and publicly available at https://zenodo.org/records/15889204. The code used in this study is available on GitHub at https://github.com/agattar/Attar_etal2025.

References

1. Kalukula Y, Stephens AD, Lammerding J *et al.* Mechanics and functional consequences of nuclear deformations. *Nat Rev Mol Cell Biol* 2022;**23**:583–602. https://doi.org/10.1038/s41580-022-00480-z
2. Miroshnikova YA, Wickström SA. Mechanical forces in nuclear organization. *Cold Spring Harb Perspect Biol* 2022;**14**:a039685. https://doi.org/10.1101/cshperspect.a039685
3. Nava MM, Miroshnikova YA, Biggs LC *et al.* Heterochromatin-driven nuclear softening protects the genome against mechanical stress-induced damage. *Cell* 2020;**181**:800–17. https://doi.org/10.1016/j.cell.2020.03.052
4. Le HQ, Ghatak S, Yeung CYC *et al.* Mechanical regulation of transcription controls Polycomb-mediated gene silencing during lineage commitment. *Nat Cell Biol* 2016;**18**:864–75. https://doi.org/10.1038/ncb3387
5. Golloshi R, Playter C, Freeman TF *et al.* Constricted migration is associated with stable 3D genome structure differences in cancer cells. *EMBO Rep* 2022;**23**:e52149.
6. Jacobson EC, Perry JK, Long DS *et al.* Migration through a small pore disrupts inactive chromatin organization in neutrophil-like cells. *BMC Biol* 2018;**16**:142.
7. Hsia CR, McAllister J, Hasan O *et al.* Confined migration induces heterochromatin formation and alters chromatin accessibility. *Iscience* 2022;**25**:104978.
8. Tajik A, Zhang Y, Wei F *et al.* Transcription upregulation via force-induced direct stretching of chromatin. *Nature Mater* 2016;**15**:1287–96.
9. Wagh K, Ishikawa M, Garcia DA *et al.* Mechanical regulation of transcription: recent advances. *Trends Cell Biol* 2021;**31**:457–72.
10. Mao Y, Wickström SA. Mechanical state transitions in the regulation of tissue form and function. *Nat Rev Mol Cell Biol* 2024;**25**:654–70.
11. Raab M, Gentili M, de Belly H *et al.* ESCRT III repairs nuclear envelope ruptures during cell migration to limit DNA damage and cell death. *Science* 2016;**352**:359–62.
12. Denais CM, Gilbert RM, Isermann P *et al.* Nuclear envelope rupture and repair during cancer cell migration. *Science* 2016;**352**:353–8.
13. Xia Y, Ivanovska IL, Zhu K *et al.* Nuclear rupture at sites of high curvature compromises retention of DNA repair factors. *J Cell Biol* 2018;**217**:3796–808.
14. Pfeifer CR, Xia Y, Zhu K *et al.* Constricted migration increases DNA damage and independently represses cell cycle. *Mol Biol Cell* 2018;**29**:1948–62.
15. Shah P, Hobson CM, Cheng S *et al.* Nuclear deformation causes DNA damage by increasing replication stress. *Curr Biol* 2021;**31**:753–65.
16. Seelbinder B, Ghosh S, Schneider SE *et al.* Nuclear deformation guides chromatin reorganization in cardiac development and disease. *Nat Biomed Eng* 2021;**5**:1500–16.
17. Gupta S, Swoger M, Saldanha R *et al.* Reorganizing chromatin by cellular deformation. *Curr Opin Cell Biol* 2024;**90**:102408.
18. Coulon A. Interphase chromatin biophysics and mechanics: new perspectives and open questions. *Curr Opin Genet Dev* 2025;**90**:102296.
19. Gibson BA, Doolittle LK, Schneider MW *et al.* Organization of chromatin by intrinsic and regulated phase separation. *Cell* 2019;**179**:470–84.
20. Strickfaden H, Tolsma TO, Sharma A *et al.* Condensed chromatin behaves like a solid on the mesoscale *in vitro* and in living cells. *Cell* 2020;**183**:1772–84.
21. Nozaki T, Imai R, Tanbo M *et al.* Dynamic organization of chromatin domains revealed by super-resolution live-cell imaging. *Mol Cell* 2017;**67**:282–93.
22. Nozaki T, Shinkai S, Ide S *et al.* Condensed but liquid-like domain organization of active chromatin regions in living human cells. *Sci Adv* 2023;**9**:eadf1488.
23. Benelli R, Weiss M. Probing local chromatin dynamics by tracking telomeres. *Biophys J* 2022;**121**:2684–92.
24. Guerrero CR, Garcia PD, Garcia R. Subsurface imaging of cell organelles by force microscopy. *ACS Nano* 2019;**13**:9629–37.
25. Keizer VI, Grosse-Holz S, Woringer M *et al.* Live-cell micromanipulation of a genomic locus reveals interphase chromatin mechanics. *Science* 2022;**377**:489–95.

26. Strom AR, Kim Y, Zhao H *et al.* Condensate interfacial forces reposition DNA loci and probe chromatin viscoelasticity. *Cell* 2024;**187**:5282–97.
27. de Vries AHB, Krenn BE, van Driel R *et al.* Direct observation of nanomechanical properties of chromatin in living cells. *Nano Lett* 2007;**7**:1424–7.
28. Stephens AD, Banigan EJ, Adam SA *et al.* Chromatin and lamin a determine two different mechanical response regimes of the cell nucleus. *Mol Biol Cell* 2017;**28**:1984–96. https://doi.org/10.1091/mbc.e16-09-0653
29. Stephens AD, Liu PZ, Banigan EJ *et al.* Chromatin histone modifications and rigidity affect nuclear morphology independent of lamins. *Mol Biol Cell* 2018;**29**:220–33. https://doi.org/10.1091/mbc.e17-06-0410
30. Stephens AD, Liu PZ, Kandula V *et al.* Physicochemical mechanotransduction alters nuclear shape and mechanics via heterochromatin formation. *Mol Biol Cell* 2019;**30**:2320–30.
31. Strom AR, Biggs RJ, Banigan EJ *et al.* HP1 is a chromatin crosslinker that controls nuclear and mitotic chromosome mechanics. *eLife* 2021;**10**:e63972. https://doi.org/10.7554/elife.63972
32. Ghosh S, Seelbinder B, Henderson JT *et al.* Deformation microscopy for dynamic intracellular and intranuclear mapping of mechanics with high spatiotemporal resolution. *Cell Rep* 2019;**27**:1607–20.
33. Bergamaschi G, Biebricher AS, Witt H *et al.* Heterogeneous force response of chromatin in isolated nuclei. *Cell Rep* 2024;**43**:114852.
34. Lherbette M, Dos Santos Á, Hari-Gupta Y *et al.* Atomic force microscopy micro-rheology reveals large structural inhomogeneities in single cell-nuclei. *Sci Rep* 2017;**7**:8116.
35. Seelbinder B, Wagner S, Jain M *et al.* Probe-free optical chromatin deformation and measurement of differential mechanical properties in the nucleus. *eLife* 2024;**13**:e76421.
36. Chalut KJ, Höpfler M, Lautenschläger F *et al.* Chromatin decondensation and nuclear softening accompany Nanog downregulation in embryonic stem cells. *Biophys J* 2012;**103**:2060–70.
37. Larson AG, Elnatan D, Keenen MM *et al.* Liquid droplet formation by HP1α suggests a role for phase separation in heterochromatin. *Nature* 2017;**547**:236–40.
38. Strom AR, Emelyanov AV, Mir M *et al.* Phase separation drives heterochromatin domain formation. *Nature* 2017;**547**:241–5.
39. Wang L, Gao Y, Zheng X *et al.* Histone modifications regulate chromatin compartmentalization by contributing to a phase separation mechanism. *Mol Cell* 2019;**76**:646–59.
40. Keenen MM, Brown D, Brennan LD *et al.* HP1 proteins compact DNA into mechanically and positionally stable phase separated domains. *eLife* 2021;**10**:e64563. https://doi.org/10.7554/elife.64563
41. Williams JF, Surovtsev IV, Schreiner SM *et al.* The condensation of HP1α/Swi6 imparts nuclear stiffness. *Cell Rep* 2024;**43**:114373.
42. Kind J, Pagie L, Ortabozkoyun H *et al.* Single-cell dynamics of genome-nuclear lamina interactions. *Cell* 2013;**153**:178–92.
43. Solovei I, Wang AS, Thanisch K *et al.* LBR and Lamin A/C sequentially tether peripheral heterochromatin and inversely regulate differentiation. *Cell* 2013;**152**:584–98. https://doi.org/10.1016/j.cell.2013.01.009
44. Poleshko A, Mansfield KM, Burlingame CC *et al.* The human protein PRR14 tethers heterochromatin to the nuclear lamina during interphase and mitotic exit. *Cell Rep* 2013;**5**:292–301. https://doi.org/10.1016/j.celrep.2013.09.024
45. Solovei I, Thanisch K, Feodorova Y. How to rule the nucleus: divide et impera. *Curr Opin Cell Biol* 2016;**40**:47–59.
46. Kirby TJ, Lammerding J. Emerging views of the nucleus as a cellular mechanosensor. *Nat Cell Biol* 2018;**20**:373–81. https://doi.org/10.1038/s41556-018-0038-y
47. Falk M, Feodorova Y, Naumova N *et al.* Heterochromatin drives compartmentalization of inverted and conventional nuclei. *Nature* 2019;**570**:395–9. https://doi.org/10.1038/s41586-019-1275-3
48. Lewis R, Sinigiani V, Koos K *et al.* LBR and LAP2 mediate heterochromatin tethering to the nuclear periphery to preserve genome homeostasis. bioRxiv, https://doi.org/10.1101/2024.12.23.628302, 23 December 2024, preprint: not peer reviewed.
49. Stephens AD, Banigan EJ, Marko JF. Chromatin's physical properties shape the nucleus and its functions. *Curr Opin Cell Biol* 2019;**58**:76–84.
50. Hsia CR, Melters DP, Dalal Y. The force is strong with this epigenome: chromatin structure and mechanobiology. *J Mol Biol* 2023;**435**:168019. https://doi.org/10.1016/j.jmb.2023.168019
51. Gerlitz G, Livnat I, Ziv C *et al.* Migration cues induce chromatin alterations. *Traffic* 2007;**8**:1521–9.
52. Gerlitz G, Bustin M. Efficient cell migration requires global chromatin condensation. *J Cell Sci* 2010;**123**:2207–17.
53. Gerlitz G. The emerging roles of heterochromatin in cell migration. *Front Cell Dev Biol* 2020;**8**:394.
54. Jost D, Carrivain P, Cavalli G *et al.* Modeling epigenome folding: formation and dynamics of topologically associated chromatin domains. *Nucleic Acids Res* 2014;**42**:9553–61.
55. Nuebler J, Fudenberg G, Imakaev M *et al.* Chromatin organization by an interplay of loop extrusion and compartmental segregation. *Proc Natl Acad Sci USA* 2018;**115**:E6697–706.
56. Chiang M, Michieletto D, Brackley CA *et al.* Polymer modeling predicts chromosome reorganization in senescence. *Cell Rep* 2019;**28**:3212–23.
57. Banigan EJ, Stephens AD, Marko JF. Mechanics and buckling of biopolymeric shells and cell nuclei. *Biophys J* 2017;**113**:1654–63. https://doi.org/10.1016/j.bpj.2017.08.034
58. Attar AG, Paturej J, Banigan EJ *et al.* Chromatin phase separation and nuclear shape fluctuations are correlated in a polymer model of the nucleus. *Nucleus* 2024;**15**:2351957. https://doi.org/10.1080/19491034.2024.2351957
59. Stefano MD, Nützmann HW, Marti-Renom MA *et al.* Polymer modelling unveils the roles of heterochromatin and nucleolar organizing regions in shaping 3D genome organization in *Arabidopsis thaliana*. *Nucleic Acids Res* 2021;**49**:1840–58. https://doi.org/10.1093/nar/gkaa1275
60. Shimi T, Pfleghaar K, Kojima S *et al.* The A- and B-type nuclear lamin networks: microdomains involved in chromatin organization and transcription. *Genes Dev* 2008;**22**:3409–21.
61. Mahamid J, Pfeffer S, Schaffer M *et al.* Visualizing the molecular sociology at the HeLa cell nuclear periphery. *Science* 2016;**351**:969–72.
62. Turgay Y, Eibauer M, Goldman AE *et al.* The molecular architecture of lamins in somatic cells. *Nature* 2017;**543**:261–4.
63. Sapra KT, Qin Z, Dubrovsky-Gaupp A *et al.* Nonlinear mechanics of lamin filaments and the meshwork topology build an emergent nuclear lamina. *Nat Commun* 2020;**11**:6205.
64. Stephens AD, Banigan EJ, Marko JF. Separate roles for chromatin and lamins in nuclear mechanics. *Nucleus* 2018;**9**:119–24. https://doi.org/10.1080/19491034.2017.1414118
65. Ou HD, Phan S, Deerinck TJ *et al.* ChromEMT: Visualizing 3D chromatin structure and compaction in interphase and mitotic cells. *Science* 2017;**357**:eaag0025.
66. Thompson AP, Aktulga HM, Berger R *et al.* LAMMPS—a flexible simulation tool for particle-based materials modeling at the atomic, meso, and continuum scales. *Comput Phys Commun* 2022;**271**:108171.
67. Stukowski A. Visualization and analysis of atomistic simulation data with OVITO—the Open Visualization Tool. *Model Simul Mater Sci Eng* 2009;**18**:015012.
68. Lieberman-Aiden E, van Berkum N, Williams L *et al.* Comprehensive mapping of long-range interactions reveals

folding principles of the human genome. *Science* 2009;**326**:289–93.

69. Shimamoto Y, Tamura S, Masumoto H *et al.* Nucleosome–nucleosome interactions via histone tails and linker DNA regulate nuclear rigidity. *Mol Biol Cell* 2017;**28**:1580–9.
70. Michieletto D, Orlandini E, Marenduzzo D. Polymer model with epigenetic recoloring reveals a pathway for the *de novo* establishment and 3D organization of chromatin domains. *Phys Rev X* 2016;**6**:041047.
71. Sanulli S, Trnka MJ, Dharmarajan V *et al.* HP1 reshapes nucleosome core to promote phase separation of heterochromatin. *Nature* 2019;**575**:390–94. https://doi.org/10.1038/s41586-019-1669-2
72. Shakya A, Park S, Rana N *et al.* Liquid–liquid phase separation of histone proteins in cells: role in chromatin organization. *Biophys J* 2020;**118**:753–64.
73. Shin S, Shi G, Thirumalai D. From effective interactions extracted using Hi-C data to chromosome structures in conventional and inverted nuclei. *PRX Life* 2023;**1**:013010. https://doi.org/10.1103/prxlife.1.013010
74. Girard M, Cruz MOdl, Marko JF *et al.* Heterochromatin flexibility contributes to chromosome segregation in the cell nucleus. *Phys Rev E* 2024;**110**:014403. https://doi.org/10.1103/PhysRevE.110.014403
75. Harr JC, Luperchio TR, Wong X *et al.* Directed targeting of chromatin to the nuclear lamina is mediated by chromatin state and A-type lamins. *J Cell Biol* 2015;**208**:33–52.
76. Steensel Bv, Belmont AS. Lamina-associated domains: links with chromosome architecture, heterochromatin, and gene repression. *Cell* 2017;**169**:780–91. https://doi.org/10.1016/j.cell.2017.04.022
77. Rubinstein M, Colby RH. Polymer physics. New York: Oxford University Press, 2003.
78. Canzio D, Chang EY, Shankar S *et al.* Chromodomain-mediated oligomerization of HP1 suggests a nucleosome-bridging mechanism for heterochromatin assembly. *Mol Cell* 2011;**41**:67–81.
79. Machida S, Takizawa Y, Ishimaru M *et al.* Structural basis of heterochromatin formation by human HP1. *Mol Cell* 2018;**69**:385–97.
80. Schreiner SM, Koo PK, Zhao Y *et al.* The tethering of chromatin to the nuclear envelope supports nuclear mechanics. *Nat Commun* 2015;**6**:7159.
81. Poleshko A, Shah PP, Gupta M *et al.* Genome-nuclear lamina interactions regulate cardiac stem cell lineage restriction. *Cell* 2017;**171**:573–87. https://doi.org/10.1016/j.cell.2017.09.018
82. Wang X, Liu H, Zhu M *et al.* Mechanical stability of the cell nucleus–roles played by the cytoskeleton in nuclear deformation and strain recovery. *J Cell Sci* 2018;**131**:jcs209627.
83. Steensel Bv, Henikoff S. Identification of *in vivo* DNA targets of chromatin proteins using tethered dam methyltransferase. *Nat Biotechnol* 2000;**18**:424–8.
84. Guelen L, Pagie L, Brasset E *et al.* Domain organization of human chromosomes revealed by mapping of nuclear lamina interactions. *Nature* 2008;**453**:948–51. https://doi.org/10.1038/nature06947
85. Eskndir N, Hossain M, Currey ML *et al.* DNA damage causes ATM-dependent heterochromatin loss leading to nuclear softening, blebbing, and rupture. *Mol Biol Cell* 2025;**36**:br6.
86. Hameed HA, Paturej J, Erbaş A. Phase behavior and dissociation kinetics of lamins in a polymer model of progeria. *J Chem Phys* 2025;**162**:185101.
87. Li Y, Lovett D, Zhang Q *et al.* Moving cell boundaries drive nuclear shaping during cell spreading. *Biophys J* 2015;**109**:670–86.
88. Tang W, Chen X, Wang X *et al.* Indentation induces instantaneous nuclear stiffening and unfolding of nuclear envelope wrinkles. *Proc Natl Acad Sci USA* 2023;**120**:e2307356120.
89. Mazumder A, Shivashankar G. Gold-nanoparticle-assisted laser perturbation of chromatin assembly reveals unusual aspects of nuclear architecture within living cells. *Biophys J* 2007;**93**:2209–16.
90. Mazumder A, Shivashankar GV. Emergence of a prestressed eukaryotic nucleus during cellular differentiation and development. *J R Soc Interface* 2010;**7**:S321–30.
91. Le Berre M, Aubertin J, Piel M. Fine control of nuclear confinement identifies a threshold deformation leading to lamina rupture and induction of specific genes. *Integr Biol* 2012;**4**:1406–14.
92. Tamiello C, Kamps MA, van den Wijngaard A *et al.* Soft substrates normalize nuclear morphology and prevent nuclear rupture in fibroblasts from a laminopathy patient with compound heterozygous LMNA mutations. *Nucleus* 2013;**4**:61–73.
93. Hatch EM, Hetzer MW. Nuclear envelope rupture is induced by actin-based nucleus confinement. *J Cell Biol* 2016;**215**:27–36.
94. Santos Á, Cook AW, Gough RE *et al.* DNA damage alters nuclear mechanics through chromatin reorganization. *Nucleic Acids Res* 2021;**49**:340–53.
95. Pho M, Berrada Y, Gunda A *et al.* Actin contraction controls nuclear blebbing and rupture independent of actin confinement. *Mol Biol Cell* 2024;**35**:ar19.
96. Liu K, Patteson AE, Banigan EJ *et al.* Dynamic nuclear structure emerges from chromatin cross-links and motors. *Phys Rev Lett* 2021;**126**:158101.
97. Berg IK, Currey ML, Gupta S *et al.* Transcription inhibition suppresses nuclear blebbing and rupture independently of nuclear rigidity. *J Cell Sci* 2023;**136**:jcs261547.
98. Lionetti MC, Bonfanti S, Fumagalli MR *et al.* Chromatin and cytoskeletal tethering determine nuclear morphology in progerin-expressing cells. *Biophys J* 2020;**118**:2319–32. https://doi.org/10.1016/j.bpj.2020.04.001
99. Hobson CM, Kern M, O'Brien III ET *et al.* Correlating nuclear morphology and external force with combined atomic force microscopy and light sheet imaging separates roles of chromatin and lamin A/C in nuclear mechanics. *Mol Biol Cell* 2020;**31**:1788–801.
100. Krause M, Te Riet J, Wolf K. Probing the compressibility of tumor cell nuclei by combined atomic force–confocal microscopy. *Phys Biol* 2013;**10**:065002.
101. Panagiotakopoulou M, Bergert M, Taubenberger A *et al.* A nanoprinted model of interstitial cancer migration reveals a link between cell deformability and proliferation. *ACS Nano* 2016;**10**:6437–48.
102. Allshire RC, Madhani HD. Ten principles of heterochromatin formation and function. *Nat Rev Mol Cell Biol* 2018;**19**:229–44.
103. van Steensel B, Furlong EE. The role of transcription in shaping the spatial organization of the genome. *Nat Rev Mol Cell Biol* 2019;**20**:327–37.
104. Belaghzal H, Borrman T, Stephens AD *et al.* Liquid chromatin Hi-C characterizes compartment-dependent chromatin interaction dynamics. *Nat Genet* 2021;**53**:367–78.
105. Khanna N, Zhang Y, Lucas JS *et al.* Chromosome dynamics near the sol-gel phase transition dictate the timing of remote genomic interactions. *Nat Commun* 2019;**10**:2771.
106. Redding S. Dynamic asymmetry and why chromatin defies simple physical definitions. *Curr Opin Cell Biol* 2021;**70**:116–22.
107. Uckelmann M, Levina V, Taveneau C *et al.* Dynamic PRC1–CBX8 stabilizes a porous structure of chromatin condensates. *Nat Struct Mol Biol* 2025;**32**:520–30.
108. Sun J, Chen J, Mohagheghian E *et al.* Force-induced gene up-regulation does not follow the weak power law but depends on H3K9 demethylation. *Sci Adv* 2020;**6**:eaay9095.

Received: April 17, 2025. **Revised:** July 17, 2025. **Editorial Decision:** July 18, 2025. **Accepted:** July 31, 2025